

# 1857 Slip on the San Andreas Fault Southeast of Cholame, California

by James J. Lienkaemper

**Abstract** Sieh and Jahns (1984) forecasted that the next moderate Parkfield earthquake might trigger a major earthquake along a fault segment greater than 30 km long southeast of Cholame. Their forecast assumed (1) the slip was 3–4 m in 1857 and characteristic of the segment; (2) a slip rate of 3.4 cm/yr; and (3) full strain release in earthquakes. This study represents an independent measurement of channel offsets, on 1:2400-scale low-sun aerial photographs and by field investigation, to estimate the amount of 1857 slip.

Although rainfall is only moderate (30 cm/yr), few reliable offsets of less than 20 m persist here because cattle grazing and agricultural disking of soft sediments on the steep terrain greatly aggravate erosion. Reconstruction of offset geometry and size depends heavily on assumptions made about the post-1857 erosion. Most of the apparent 3- to 4-m offsets of Sieh and Jahns (1984) can also be measured as 2 to 3 m larger with equal or lower uncertainty. The four offsets judged as most reliable range between 5.4 and 6.7 m, and the 11 offsets of medium-high reliability average  $5.8 \pm 0.3$  m.

Data are too sparse and ambiguous to resolve details of the 1857 slip for this segment but it is distinctly less than the 9 m of the Carrizo Plain and more than the 3–4 m previously estimated. Further trenching may refine some measurements, but probability calculations for a Cholame segment earthquake must allow for large observer-dependent uncertainty in the 1857 slip. Although the probability of an  $M \geq 7$  Cholame event seems less than that suggested by a 3.5-m characteristic earthquake model, it remains among the highest in the state.

## Introduction

Sieh and Jahns (1984) proposed a Cholame segment of the San Andreas fault capable of producing major ( $M \geq 7$ ) earthquakes that extend southeastward from the 1966 Parkfield rupture segment to the northern part of the Carrizo Plain (Fig. 1). Although this segment has remained locked since 1857, it is of considerable scientific and public interest because it lies adjacent to a segment where moderate ( $M$  5.5–6) earthquakes occur frequently. Foreshocks occurred near Parkfield in the hours preceding the 1857 event (Sieh, 1978a). This suggests that if stress conditions are favorable a moderate Parkfield event could possibly trigger or grow into much larger events (Agnew and Sieh, 1978; Sieh and Jahns, 1984). If a typical Parkfield event were to trigger or precede larger ( $M \geq 7$ ) events to the south, future Parkfield events could constitute a far greater hazard to the public.

Sieh and Jahns (1984) estimated from stream offsets that the 1857 slip was 3–4 m along the 30-km-long part of the fault southward of Cholame. From this, they argued that a 90-km segment from Cholame to Carrizo Plain “. . . is likely to generate a major earthquake by the turn of the century.” In evaluating the post-1857 slip deficit, Lienkaemper and Prescott (1989) agreed with Sieh and Jahns that much of the

1966 Parkfield rupture segment has a large deficit in surface slip. This deficit is too large to be relieved by creep and Parkfield earthquakes alone, and it probably exceeds 4 m southward of Cholame. Thus, the seismic potential for an  $M$  7 event already exists. If the Cholame segment slips 3–4 m in characteristic earthquakes, then the probability of it cascading or triggering from the next Parkfield event would indeed be high.

In 1986–1988, Lienkaemper investigated stream channel offsets on the Cholame segment with the intent of reproducing and augmenting the existing data set. The goal was to test the reliability of the 3–4 m-estimate of the 1857 slip that Sieh and Jahns (1984) had suggested might be the characteristic slip for the Cholame segment. From the initial observations, Lienkaemper (1987) and Lienkaemper and Sturm (1989) concluded that the slip in 1857 probably averaged ca. 6 m, considerably larger than 3–4 m.

Faced with these contradictory results, the Working Group on California Earthquake Probabilities (WGCEP88, 1988) calculated 30-yr probabilities of  $M$  7 earthquakes on this segment for both estimates of slip. Resulting probabilities were 0.5 using the 3.5-m slip after Sieh (1978b) and

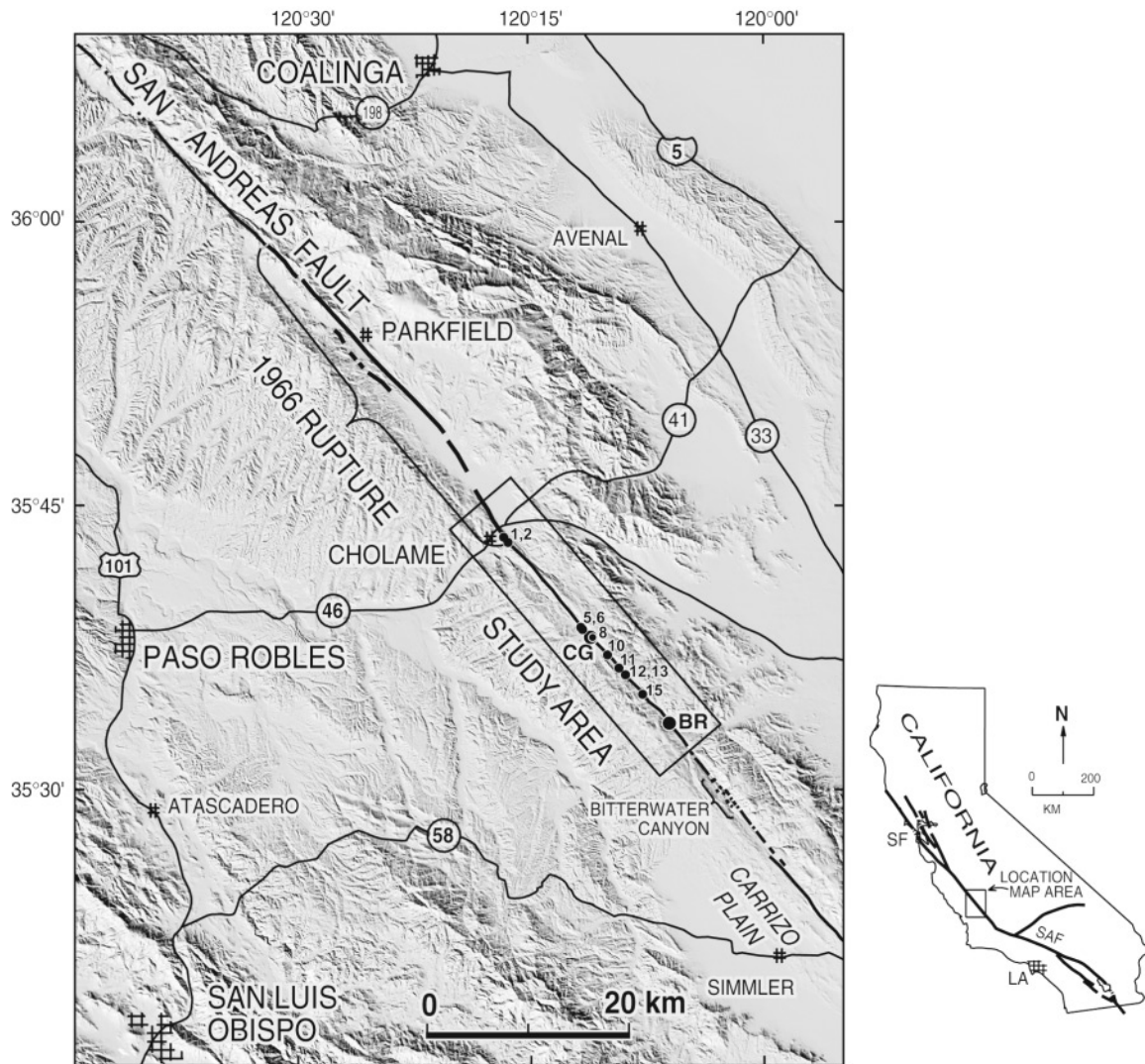


Figure 1. Map showing section of the San Andreas fault investigated for this study, between Cholame and Bitterwater Canyon. Offset channel locations (Tables 1 and 2) given as distances from BR, Bitterwater Road. CG, Carter Grade. Numbers along fault are key sites, numbered after Sieh (1978b).

0.2 using the 6-m slip after Lienkaemper (1987). They settled on a probability of 0.3 based on an average of the two slip estimates (4.75 m). If one assumes that this segment is ready to rupture once slip deficit exceeds the slip in the last event, then the probability of generating a major earthquake remains high regardless of any ambiguities in the interpretation of the 1857 slip. The expected recurrence interval based on the Sieh and Jahns slip estimate is quite short at 103 yr (3.5 m/3.4 cm/yr) compared to 170 yr based on this study (5.8 m/3.4 cm/yr). Hence, the latter mean return time (2027 = 1857 + 170 yr) falls within the current 30-yr window, whereas the former estimate (1960 = 1857 + 103 yr) is receding from the window. Thus, the 30-yr probability based on the 6-m slip is growing while that based on the 3.5-m slip is shrinking. Although calculated probabilities will vary depending on the assumed probability model, they

remain similar to those of WGCEP88, but with a reversal of their probabilities (i.e., the 6-m slip now yields higher probabilities and the 3.5-m slip, lower probabilities). Consequently, this segment remains among the most likely fault segments to generate major earthquakes in California in the near future.

Similar moderate earthquakes seemed to occur near Parkfield every  $22 \pm 3$  yr, based on linear regression of events in 1857, 1881, 1901, 1922, 1934, and 1966 (Bakun and McEvilly, 1984; Bakun and Lindh, 1985b; Stuart *et al.*, 1985). Thus, the U.S. Geological Survey (USGS) forecast that the next such event would occur by  $1988 \pm 5$  yr (0.95 confidence). This forecast led to a program of scientific research and monitoring for possible earthquake precursors called the Parkfield Earthquake Prediction Experiment (Bakun and Lindh, 1985a; Bakun *et al.*, 1987). The Exper-

Table 1  
Small Offsets (<20-m slip)

Site*	Distance (km) <sup>†</sup>	Slip (m)	Reliability	Comments
147a	-2.46	0 ± 1	Low	Gully weakly incised into a grading fan that conceals fault.
147b	-2.37	0 ± 0.2	Med	Fresh gullies into Holocene fan deposits.
147c	-2.14	10 ± 2	Med	Apparent offset of 12 ± 0.5 m corrected for diskings effects.
145a	-1.69	6.7 ± 0.5	High	In 1966 aerial photos offset unusually distinct. Channel straight and parallel near fault. Offset since destroyed by diskings.
143a	-1.35	0 ± 0.5	Med	New tail after 1857 event; old one beheaded and destroyed.
	0.00			<i>Bitterwater Road</i>
122a:15	3.91	5.5 ± 0.7	High	Gully in late Holocene fan; offset measured on 1966 aerial photos. Post-1966 diskings reduced apparent offset to 3.5 m.
113c2	5.92	5 ± 1	Low	Located 200 m north of TWR1 creepmeter. Other traces here probably have equal or greater slip, but offsets badly eroded.
113c1		11 ± 2	Low	
109a:14	6.41	?	Low	Slip could be 0 or 6 m. Curved gully heavily eroded at fault.
109c:13	6.61	4 ± 4	Low	Landslide head scarp may be offset. Fault location uncertain and head scarp too irregular for certain interpretation.
109d:12	6.69	4.5 ± 1.5	Med	Slumping southeast of head near fault trace makes interpretations ambiguous.
107a	6.95	8 ± 2	Low	Short segments at low angle to fault; possible second trace.
107b	7.05	6 ± 2	Med	Clear offset, but second fault trace possibly still active.
107c	7.11	4.6 ± 1	Low	Small gully, weakly incised; possible second trace.
107d	7.12	5.5 ± 1	Low	Small gully, weakly incised; possible second trace.
107g:11	7.31	6.2 ± 0.7	Med	Main trace (4.2 ± 0.6); second trace offsets measured on bases of both banks of large channel (2.0 ± 0.3). Second trace trenched in 1988 yielding a modern radiocarbon date from peat in the fault fissure (i.e., last event was almost certainly 1857).
105a	7.41	5 ± 2	Low	Tail wider than head and offset obscured by colluvium.
99a2:10	9.01	6 ± 3	Low	Three active traces offset deeply-eroded, wide, sinuous channel.
99a1	9.01	17 ± 6	High	Head and tail straight and parallel at scale of offset wide, lobate soil slump.
97b	9.55	0 ± 0.8	High	Deeply cut gully not yet incised in 1930, 1942, and 1966 photos.
97d1	9.88	15 ± 5	Med	Intense and irregular erosion near fault causes large uncertainty.
95a	9.97	4.9 ± 1.7	Med	Straight channel, but its width causes large range in slip estimated from 1966 aerial photos. Considerable erosion since 1966 prevents remeasurement.
89c:9	11.24	8 ± 4	Low	Short, wide, sinuous channel. Two other traces active here, but not included.
	11.39			<i>Carter Grade</i>
84a3:8	12.28	5.4 ± 0.5	High	Unusually straight head, but tail sinuous. Rock outcrops at fault trace complicate interpretation.
b2:7	12.52	6 ± 3	Low	Tail direction greatly askew from head near fault. Badland erosion makes exact reconstruction impossible.
b1	12.53	15 ± 5	Low	Slightly clearer than smaller offset here, but intense erosion prevents certain reconstruction.
82a:6	12.67	5.5 ± 3.5	Low	Severe erosion and slumping near fault allow many possible reconstructions of slip from highly askew head and tail.
b	12.79	4.9 ± 1.4	Low	Sum of offset on two poorly incised channels across two poorly expressed fault traces.
c,d:5	12.86	5.3 ± 1.2	Low	Average of total slip on two gullies offset on main and splay faults. Rocky tail segment on 82c makes favored interpretation nonunique. Difficult to estimate uncertainty numerically because of channel complexity.
e	12.93	13 ± 5	Med	Head and tail parallel, but heavy erosion at fault trace makes amount of offset inexact.
80c	13.30	10 ± 5	Low	Slip on active splay fault not included. Straight head permits offset interpretation, but tail may be captured, thus apparent offset may not represent fault slip.
43b	20.82	12 ± 3	Med	Distinct offset of straight head, but exact shape of tail obscured by landsliding and erosion.
c	20.86	0.6 ± 0.6	High	Deeply incised straight gullies (c and d). Each has large alluvial fan deposited on nearby modern fluvial terrace.
d	20.94	0.8 ± 0.8	High	
e	21.02	6.8 ± 1.5	Med	Straight head; tail probably parallel but degraded near fault.
f:4	21.18	5.4 ± 2.2	Low	Offset distinctly tectonic, but head and tail curved. Extreme erosion near fault makes many reconstructions plausible.
35a3:3	22.92	6.6 ± 3	Low	Various offset reconstructions are plausible: one likely history involves tail capture that invalidates slip interpretation.

(continued)

Table 1 (Continued)  
Small Offsets (<20-m slip)

Site <sup>a</sup>	Distance (km) <sup>†</sup>	Slip (m)	Reliability	Comments
33b4	23.46	5.7 ± 2	Med	Head and tail straight, but misaligned by 8°. Recent entrenchment (probably from artificially lowered base level of nearby borrow pit) has straightened offset within ± 15 m of fault.
31a:2	23.74	6.2 ± 0.9	High	Narrow, straight gully. Most distinct and best preserved small offset between Cholame Valley and Bitterwater Canyon.
29a1	24.16	13 ± 2	High	Narrow, steep, and straight gully. Head and tail nearly parallel.
a2	24.17	1.4 ± 0.8	Med	Same head as 29a1. Offset now less clear than in 1966 aerial photos.
b2:1	24.38	1.1 ± 0.2	Med	Both head and tail narrow, straight, and parallel within 1.5°. Fault offset covered by 8-m-wide, lobate soil slump.
	25.55			<i>Highway 46</i>
17a	26.94	4.7 ± 0.9	Med	Straight and narrow head; sinuous and broad tail. Offset measured on 1:1500-scale, post-1966 earthquake photos; site much degraded now. Gully at scissor point: uplift northwest of head, subsidence to southeast. Head incised and realigned near offset probably result of presumed large 1857 vertical slip here. Small slump obscures part of tail. Error reflects one standard deviation of various reasonable channel wall and centerline projections to the fault.
12b:0	28.16	0.3 ± 0.2	Med	Narrow, straight gully. Accuracy limited by minor curvature in head and straightening of offset within 2–3 m of fault
12c:0	28.17	1.3 ± 0.3	High	Narrow, straight, parallel head and tail of small gully. Post-earthquake aerial photo (1:1600) shows 1966 rupture between two offset segments with well-defined centers.
12d	28.30	0.7 ± 0.3	Med	Straight, narrow head has well-defined center, but less than 1 m of tail lies northeast of 1966 fracture zone, thus slip probably reflects a minimum because of unknown amount of straightening and distributed shear northeast of 2-m-wide zone of cracks.

<sup>a</sup>USGS Cholame (1:2400) aerial photo frame number; letter assigned to each offset headwater; subscript given to additional offset tails. Number in boldface after colon, site number of Sieh (1978b).

<sup>†</sup>Distance from Bitterwater Road along fault strike (N319°E).

iment was accompanied by a public earthquake preparedness effort by the California Office of Emergency Services (Andrews, 1992; California OES, 1988). With the review and approval of the National Earthquake Prediction Evaluation Council (NEPEC), the Parkfield Experiment developed scientific criteria to declare various levels of public alert in terms of probability of occurrence in 72 hr. The NEPEC considered the possibility of an *M* 7 Cholame rupture but did not calculate its probability or establish alert criteria for it. However, the highest [A] level alert included the following language for the director of OES (California OES, 1988): “[a *M* 7 Cholame event] . . . is sufficiently plausible geologically to warrant consideration in emergency planning and response.”

After the prediction window closed in 1993, many workers reviewed or re-evaluated both the physical and the statistical models underlying the supposed regular recurrence of Parkfield events (Davis *et al.*, 1988; Savage, 1991, 1993; Ben-Zion *et al.*, 1993; NEPECWG, 1994; Roeloffs and Langbein, 1994; Lindh and Lim, 1995; Miller, 1996; Kagan, 1997; Jackson and Kagan, 1998; Michael and Jones, 1998). In addition to reviewing and modifying the prediction model and alert procedures (Michael and Jones, 1998), others have reviewed and reaffirmed the plausibility of *M* 7+ Cholame earthquakes (Arrowsmith *et al.*, 1997). Although the original prediction hypothesis failed scaled-back

scientific monitoring and emergency preparedness efforts continue in Parkfield.

The Parkfield segment forms a major transition in surface-slip behavior on the San Andreas fault. To the north, slip occurs as fault creep at the surface, that is steadily, aseismically, and at rates similar to the long-term slip rate (ca. 3 cm/yr). To the south, no surface creep is observed (<0.1 cm/yr; Brown and Wallace, 1968; Burford and Harsh, 1980). Surface slip south of the Parkfield segment last occurred during the 1857 earthquake (Sieh, 1978b). Although no contemporary measurements of the 1857 slip exist, Johnson (1905) shows a crude sketch of a 100 by 150-ft corral near Cholame with two sides right-laterally offset. These offsets scale to ca. 7 ± 2.5 m. This account does suggest considerable slip here in 1857 but cannot be taken too literally.

In the mid-1970s, Sieh (1978b) did the first comprehensive study of the slip associated with the great 1857 earthquake. He measured more than 150 offset geomorphic features, principally the smallest stream channel offsets, along a 350-km reach of the fault between Cholame and Wrightwood. This included 16 sites along the Cholame segment. Sieh and Jahns (1984) reported additional 1857 offsets but none were along the Cholame segment. Sieh (1978b) generally spent at least 15 min. at each site measuring offsets by tape measure and produced plane-table maps at many sites. He described the reliability for each offset measure-

Table 2  
Large Offsets (>20-m slip)

Site <sup>a</sup>	Distance (km) <sup>b</sup>	Slip (m)	Reliability	Comments
	0.00			<i>Bitterwater Road</i>
115a1	5.21	80 ± 15	Low	Long-abandoned, beheaded tail
115a2	5.25	40 ± 20	Low	Active tail. Both a1 and a2 might have been captured tails of other channels to the southeast, thus invalid for slip.
115b	5.40	40 ± 10	High	Broad alluviated canyon. Trenched for slip rate by K. E. Sieh (Personal comm. 1986), but stratigraphy destroyed by bioturbation.
113a	5.60	45 ± 10	Med	Deeply incised channel 110 m southeast of Twisselmann Ranch creepmeter. Incision probably since cattle introduced.
113b	5.83	145 ± 40	Med	Includes slip on two traces. Head broad and gently curved; tail straight and deeply incised. About 160 m northwest of creepmeter.
111a	6.20	180 ± 40	Low	Large drainage crosses fault at low angle. Tail diverted by artificial levee between 1930 and 1966.
109b	6.57	35 ± 10	Med	Ostensibly clear match of head and tail complicated by contradictory age relationship with large landslide. Sole of seemingly less-offset landslide (see 14c:13, Table 1) exposed in channel wall.
109d	6.79	40 ± 20	Med	Landslide has covered much of tail. Heavy erosion of large head near fault further reduces accuracy in projecting offset.
107e	7.16	70 ± 10	Med	Head and tail match looks reasonable, but second trace that looks inactive now not included, possibly active during part of this offset, thus total slip is a minimum.
107f	7.29	70 ± 10	High	Offset on both main fault and splay included. Head and tail unusually straight and parallel to each other.
105b	7.47	27 ± 4	High	Beheaded. Excellent match of straight and narrow head and tail parallel to each other.
105c	7.66	120 ± 20	Med	Slip summed over two traces (100 ± 15 m on main fault; 20 ± 15 m on secondary parallel trace). Youthful surface expression shows secondary trace distinctly active, but curvature of tail near fault makes amount of slip unclear.
105d	7.87	110 ± 20	High	Long-abandoned beheaded tail matches broad, straight head filled deeply with alluvium.
103a	7.90	120 ± 30	Med	Low-angle intersection with fault and possibility of activity on second trace reduce reliability of slip.
103b	7.99	45 ± 3	High	Head and tail of large drainage unusually straight, narrow, and parallel to each other. Single, narrow, distinct fault trace.
99b	9.05	40 ± 10	Med	Large channel reliably matched across fault, but heavy erosion of tail and wide zone of faulting makes projection of offset inexact.
99c	9.21	75 ± 20	Med	Precise original position of head uncertain because of burial by shutterridge-ponded debris.
99d	9.33	65 ± 15	Med	Tail abandoned because head captured by 99c. Straight head (except for part subjected to shutterridge ponding) allows reasonable reconstruction.
99e	9.41	30 ± 15	Low	Straight tail, but curvature of head constrains slip poorly.
97a2	9.56	60 ± 10	High	Large, narrow straight head distinctly matches parallel tail.
97a1	9.65	115 ± 15	High	Straight parallel tail similarly well matched to same head-97a, but beheaded long ago.
97c	9.78	80 ± 20	Med	Sum of offset on two traces. Head straight, but tail poorly defined. Not certain that secondary trace is still active.
97d1	9.89	60 ± 5	High	Tail straight, narrow and parallel to head. Unusually exact reconstruction of long beheaded tail. Alluvial cone of d1 nearly all buried by that of d2.
95b	10.14	70 ± 25	Med	Offset on two active traces (50 m, 20 m). Main offset measured on 1930 photograph because site since covered by debris from massive landsliding.
95c	10.26	160 ± 30	Med	Long-abandoned straight tail offset from straight head (13° from parallel to each other). Measured on 1930 air photo because head since destroyed by massive landslide.
93a2	10.49	25 ± 10	Med	Straight head, but deeply eroded broad tail causes low accuracy in measurement. Use 1930 and 1966 aerial photos to measure. Site has since been altered by major landsliding and construction of stock pond.
a1	10.72	325 ± 30	Med	Drainage from head 93a maintained its path along the fault to 93a1 for several millennia until 93a2 formed and caused abandonment. Use 1930 and 1966 photos for head.
89a3	11.22	175 ± 25	Med	Large drainage crosses three active fault strands. Unusually straight and parallel head and tail allow measurement of offset by projecting channel centers across all three fault traces.
	11.39			<i>Carter Grade</i>
89a2	11.41	350 ± 40	Low	Both 89a2 and 89a1 probably tails of 89a, but possible alternative head exists, thus reliability judged low.
89a1	11.64	600 ± 50	Low	
84a2	12.33	50 ± 10	Med	Both 84a2 and 84a1, abandoned tails of straight, narrow head 84a.

(continued)

Table 2 (Continued)  
Large Offsets (>20-m slip)

Site*	Distance (km) <sup>†</sup>	Slip (m)	Reliability	Comments
84a1	12.41	130 ± 10	Med	As stream gradient along fault lowered, over-topping of shutterridge cut new outlets; latest tail, 84a3, see Table 1.
80a	13.09	45 ± 10	Med	Sum of slip across 3 active traces on straight, nearly parallel segments. Assigned arbitrarily large error bar because intense erosion occurred, thus simplicity of reconstruction may be fortuitous.
80b	13.14	45 ± 10	Low	Slip on main trace only. One minor secondary trace not included. A third trace may have considerable slip or alternatively may only deflect drainage, and represents no slip.
45a	20.76	40 ± 10	Med	Head and toe of landslide offset by single narrow fault trace. Northwest and southeast edges of ring-shaped slide displaced same amount.
41a3	21.72	30 ± 10	Med	A classic succession of three abandoned tails: 41a1, a2 and a3. Next major earthquake will behead present active tail, a3. Straight, narrow and unusually parallel head and tails make reconstructions certain, except a3 requires long projection of channel center through landslide debris at fault.
41a2	21.76	115 ± 10	High	
41a1	21.84	160 ± 10	High	
35a1	22.68	215 ± 20	Med	Long-abandoned, deeply eroded tail captured two new heads. Initial head (35a), large, straight drainage clearly matches tails a1 and a2.
35a2	22.84	70 ± 10	Med	Short abandoned tail now wind gap. Error estimate based on possible range of drift in head channel center from post-offset incision.
35b	22.92	54 ± 5	Med	Match of head and tail most probably correct, but interaction with much larger head 35a obscures some details of offset.
35c	23.04	82 ± 5	High	Especially good matches of straight, narrow, and parallel head and tail. Proximity of rapidly incising major drainage continues to reduce local base level and prevents abandonment of this tail.
33a1	23.23	30 ± 6	Med	Good matches of straight, parallel head and tail. Head captured by other outlet. Southeast wall of abandoned tail carried away by landslide. Reconstruction assumes tail was shaped like head.
33b1	23.34	120 ± 15	Med	Long-abandoned tail captured by 33a. Straight head; uncertainty mostly from effect of capture causing flow from another direction.
33b3	23.43	30 ± 5	Med	Intermediate tail b2 offset 90 m ignored because too poorly expressed. Tail b3, straight and well preserved because completely abandoned; escaped deep incision experience by head by artificial base-level change (see Table 1, 33b4).
31c	23.96	100 ± 25	Med	Head 31c, large drainage 30-m southeast of USGS creepmeter X461. Original center of head channel uncertain because of its breadth and effects of badland erosion. Flow from adjacent head to southeast, 31b, overprinted tail of 31c. Match of head and tail probably reflects true slip, but straight head and tail not parallel, hence large error and reduced reliability.
29b1	24.35	33 ± 3	High	Abandoned tail of Sieh (1978) site 1. Straight and narrow head. All error in offset estimate from breadth of tail. Fault trace narrow and well defined.
	25.55			Highway 46

\*USGS Cholame (1:2400) aerial photo frame number; letter assigned to each offset headwater; subscript given to additional offset tails.

<sup>†</sup>Distance from Bitterwater Road along fault strike (N319°E).

ment as: Poor (P), (P/F), Fair (F), (F/G), Good (G), (G/Exc), and Excellent (Exc). Sieh and Jahns (1984) based their proposed 3 to 4-m characteristic slip of the Cholame segment on offsets at eight sites of Sieh (1978b), excluding only the lowest-ranked (P and P/F) data. Lienkaemper remeasured all the 16 small stream offsets (<20 m) measured by Sieh along the Cholame segment and added 26 others (Table 1). Additionally, he measured 47 larger (>20 m) offsets hoping to infer any possible recurrence of characteristic slip events and to gain an understanding of the longevity of stream offsets (Table 2).

The goal of this article is to present and explain these observations of channel offset and to clarify how these mea-

surements differ from those of Sieh (1978b) at the eight sites selected by Sieh and Jahns (1984). Hence, we begin with a brief discussion of the methodology employed, especially as to how it differs from that of Sieh (1978b). Next, we present the results, beginning with the channels that we agree are the most reliable and then proceed toward those we agree to be less reliable. Finally, we give a description of the data from new sites, that is, data not previously reported in Sieh (1978b), and a summary all of those data believed to best constrain the 1857 slip and might characterize a Cholame segment. Supplementary documentation, 3D imagery of selected sites, is on line at <http://quake.wr.usgs.gov/docs/deformation/cholame1857/> (URL).

## Methodology

Like Sieh (1978b), the search for offset channels began on USGS WRD aerial photos taken in 1966 (1:6000 scale). These photos allowed identification of sites for more detailed work and for the production of precise topographic maps (e.g., Fig. 2) (method described in Lienkaemper and Sturm, 1989). Detailed maps of key offsets were produced photogrammetrically, and a detailed analysis was made of each offset using a mirror stereoscope on new low-sun-angle, high-resolution, aerial photographs of the Cholame segment taken in 1986 (USGS Cholame, 1:2400 scale). Surveyed ground control at several sites and the maintenance of prescribed altitudes during the photography assured scaling accuracy at all sites. Topographic map features and elevations gave additional control to check photo scale and accurately determine local scale.

After a surface rupture offsets a channel, the channel immediately begins to straighten itself at the fault because erosion and colluviation is most intense there. After many decades the straightening and colluviation can greatly obscure the original amount of offset, generally making it appear smaller, because the eye integrates the straightening reaches near the fault with the distal reaches of the stream. All the 1857 offset channels are now straightened over several meters. With each major storm they become even

straighter. On aerial photos one can easily view the entire length of an offset gully at nearly uniform scale, whereas a ground observer standing on the fault observes in detail only the few meters of the channel nearest the fault. Beyond this close range, the view along the centerline of a channel is strongly foreshortened simply as a characteristic of human scale. Because field observations can vary considerably with changing perspectives, greater weight is placed on detailed photo analysis. However, Lienkaemper also made field measurements of offset in the manner of Sieh (1987b) (i.e., by standing at the fault trace). When field observations of offsets include the additional rigor of flagging exact centers (thalwegs) at uniform intervals outside the zone of straightening, field observations and photo analyses tend to agree closely. The general assumption made in most analyses is that the head (above the fault) and tail (below the fault) of the stream channel were originally nearly straight and parallel near a single, narrow fault trace (e.g., Fig. 2). The quantitative uncertainties ( $\pm$ ) given in Table 1 reflect the full range of offset interpretations considered reasonable. Generally, the more parallel and straight the channel, the lower the uncertainty. Sites with channels having straight and parallel reaches above and below the fault and no major complications rank high in reliability. Where major ambiguities in interpretation arise from multiple fault traces, sinuous thalwegs, or erosional and slumping modifications, the site

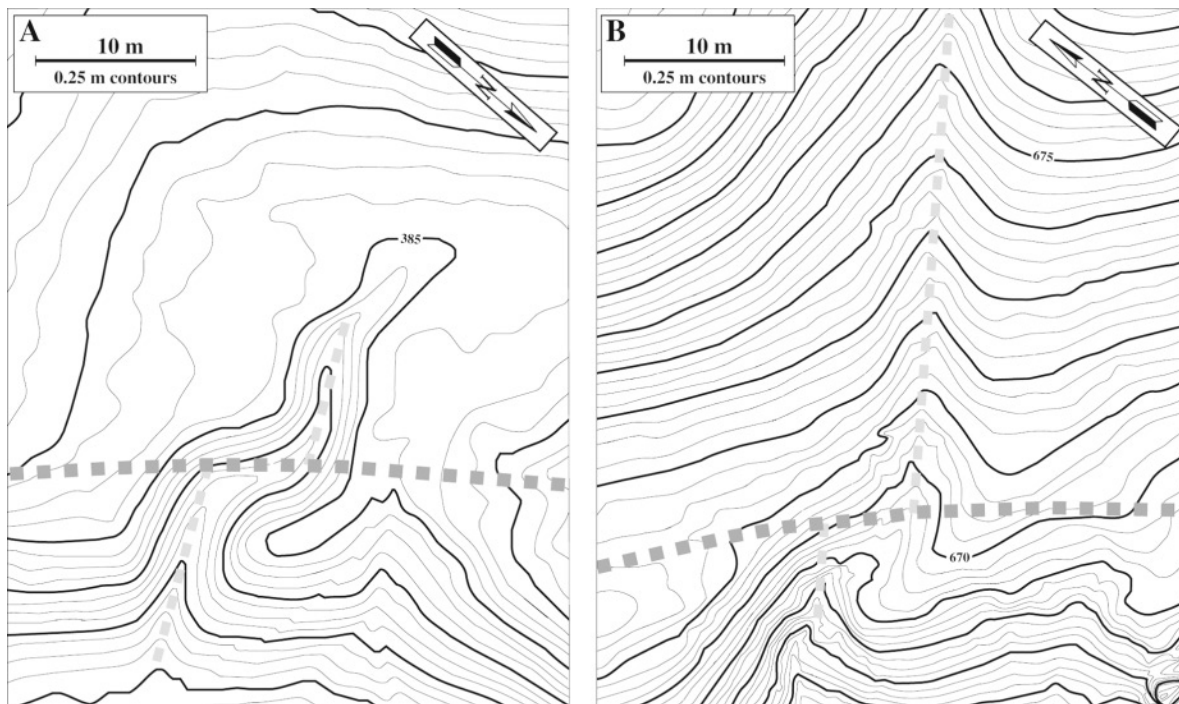


Figure 2. Topographic maps of two sites made using high-precision photogrammetry and 1:2400 aerial photos with precisely surveyed ground control (Lienkaemper and Sturm, 1989). Darker dashed line, San Andreas fault; lighter dashed line, best-fit offset-channel interpretations (assumes original channel centers are parallel directly above and below fault). (A) 31a:2 (slip  $6.2 \pm 0.9$  m); (B) 84a:3:8 (slip  $5.4 \pm 0.5$  m), that is, sites 2 and 8 of Sieh (1978). North arrows are approximate.

ranks low in reliability. Sites of moderate reliability have some complication but are otherwise worth further consideration to resolve ambiguities. The ranking process rejects (i.e., ranks as low reliability) a much greater proportion of sites than rejected by Sieh (1978b). Presumably, more are rejected because this study includes nearly three times the total number of observations and thus could better afford to reject poor sites.

Table 1 shows the summary descriptions for small (<20 m) offsets examined in this investigation. They are tabulated

for a ca. 30-km section of the fault that starts at the southeast end of the study area near Bitterwater Road (BR, Fig. 1) and ends near Cholame (and Highway 46). Site numbers (e.g., 99a2:10) refer to a frame (e.g., 99) of USGS Cholame aerial photos and have a letter (e.g., a) that indicates the order of the offset channel head in that frame starting from the southeast corner. Additional numbers indicate additional tails (e.g., 2, this is the second tail to head 99a). Finally, bold numbers following a colon (e.g., :10) indicate that this site was described as site 10 by Sieh (1978b).

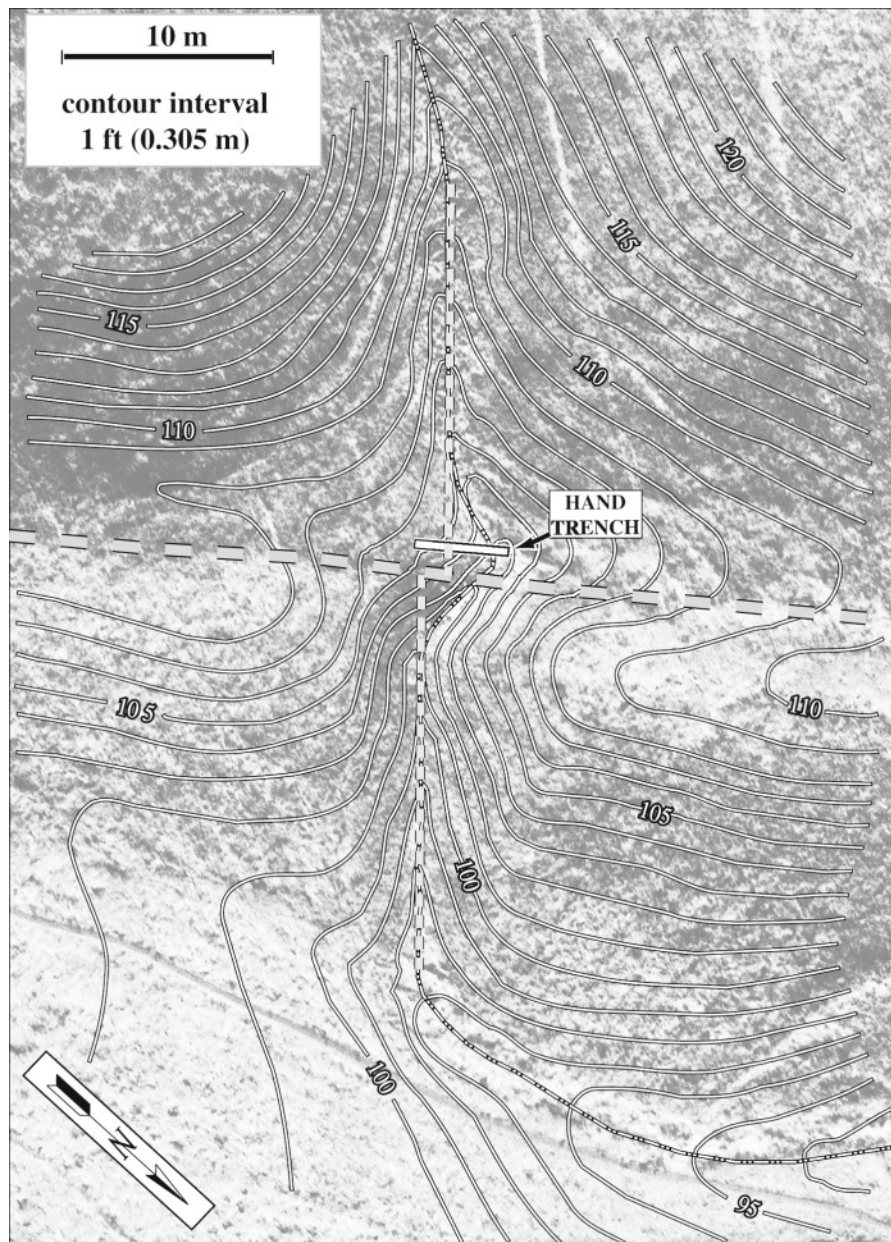


Figure 3. Topographic map of site 29b2:1 (slip  $1.1 \pm 0.2$  m), that is, site 1 of Sieh (1978b). Contours (in white) of Sieh (1978b) made using plane table, superimposed on 1:2400 low-sun-angle, aerial photo image. Fault and offset indicated as in Figure 2. Hand-trench log shown in Figure 5A.

## Results

Data follow in descending order of agreement between this investigation and Sieh (1978b), with reference to our respective reliability rankings and the applicability of each channel to the 1857 slip. First, let us consider the following four of the eight sites used by Sieh and Jahns (1984) to characterize the 1857 slip on the Cholame segment: 122a:15, 29b2:1, 107g:11, and 109d:12. These sites, Sieh and Lienkaemper both rank as reliable indicators of slip, if not necessarily the 1857 slip. Both assigned the highest reliability ranking to site 122a:15. Sieh (1978b) and Lienkaemper both believe that it represents the 1857 slip and can be measured with great reliability. However, they disagreed considerably on the amount of slip, and this site was by itself the subject of an earlier article (Lienkaemper and Sturm, 1989). The channel had seriously degraded between 1966 and 1986 as shown in detailed photogrammetric analysis. An offset of  $5.7 \pm 0.7$  m, evident in the 1966 photos, appears as a  $3.5 \pm 0.5$ -m offset in the 1986 photos. It still looked like a reliable offset but it does not reflect the 1857 slip. This change in apparent offset occurred because a steep left bank of the stream was much more vulnerable to agricultural disking along its head than along its tail.

Lienkaemper agreed with Sieh (1978b) that offsets at sites 31a:2 and 84a3:8 are reliable (Fig. 2) and that slip is large at these sites, ca. 5–7 m. Lienkaemper suggested that this slip is from 1857 alone, whereas Sieh (1978b) inferred that it accumulated from 1857 and a previous large event. Thus, these two sites were not included in the eight key sites for 1857 of Sieh and Jahns (1984). Such a disagreement can probably be resolved best by the full evaluation of what range of slip, if any, seems to dominate the Cholame segment (e.g., 3–4 versus 5–7 m).

Both agree that 29b2:1 and 107g:11 can yield reliable offsets (Figs. 3–5), but Lienkaemper concluded that they suffer from complications that required clarification. Site 29b2:1 shows the most remarkably parallel head and tail of any small stream offset ( $1.1 \pm 0.2$  m; Table 1) in the entire ca. 30-km Cholame study area. However, within a few meters of the fault, colluviation or soil creep has placed a lobe of soil over the original thalweg (buried thalweg in Fig. 5A). This buried thalweg contains the minor coarse bed load to be expected in this environment, has curvature similar to the exposed channel, and trends parallel to and is aligned ( $\pm 0.5$  m) with the head of the channel above the soil lobe. In fact, the trench showed that the buried thalweg suggests even less accumulated slip, ca. 0.5 m. Diversion around this lobe (see surface thalweg in Fig. 5B) makes possible the perception of larger offset (e.g.,  $3.5 \pm 0.2$  m in Sieh [1978b]).

Was there only 1 m of the 1857 slip here? Probably not; it is much more likely that this channel was reincised at the fault, as explained by Sieh (1978b), but after 1857. The slip from creep and Parkfield earthquake ruptures after 1857 is enough to explain this small offset. The nearest complete measurement of the 1966 slip was made 1 km to the north

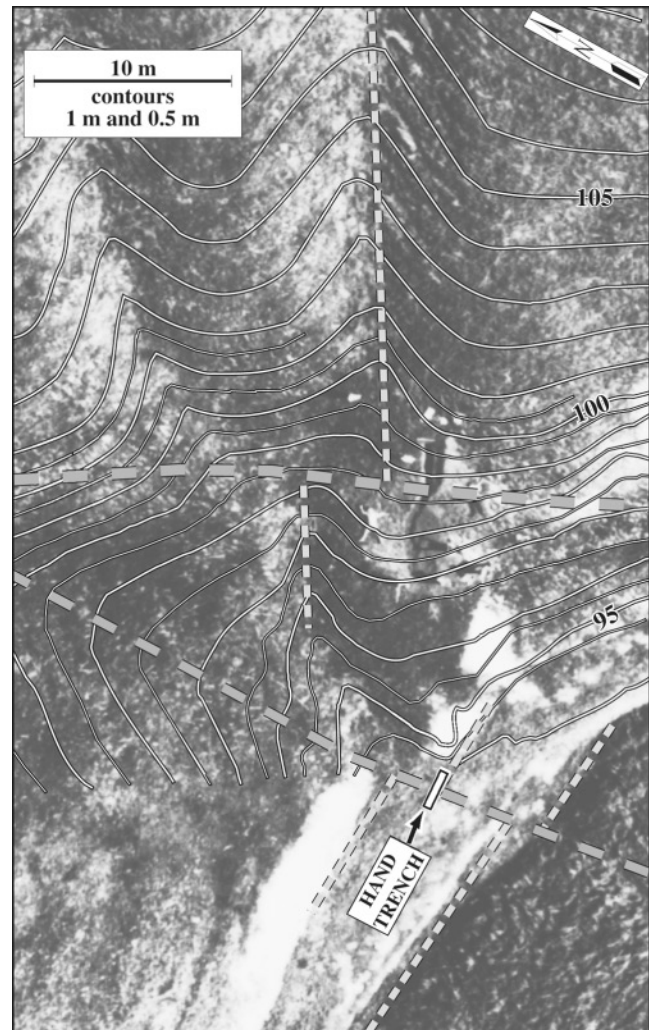


Figure 4. Topographic map of site 107g:11 (slip  $6.2 \pm 0.7$  m), that is site 11 of Sieh (1978). Contours (in white) of Sieh (1978b) made using plane table, superimposed on 1:2400 low-sun-angle, aerial photo image. A 3D image of the site is available at the URL. Fault and offset indicated as in Figure 2. Hand trench of second fault trace, log shown in Figure 5B.

at Highway 46. There creep averages ca. 0.0036 m/yr and showed 0.13 m of slip in the 1966 Parkfield rupture, which extended yet another 5.8 km to the south (Lienkaemper and Prescott, 1989), well south of 29b2:1. So, regardless of channel interpretation, since 1857 the slip here has accrued from as many as five Parkfield events (1881, 1901, 1922, 1934, 1966) and 130 yr of creeping. We compute a total possible post-1857 slip of  $1.12 \text{ m} = (5 \times 0.13) + (130 \times 0.0036)$ . Thus, the less than 1-m offset observed at 29b2:1 can be better explained as an accumulation of slip from creep and Parkfield events over many decades, rather than as a result of 1857 slip. In conclusion, this new tail of the gully was most likely incised after 1857 and thus is not used to estimate 1857 slip in this study.

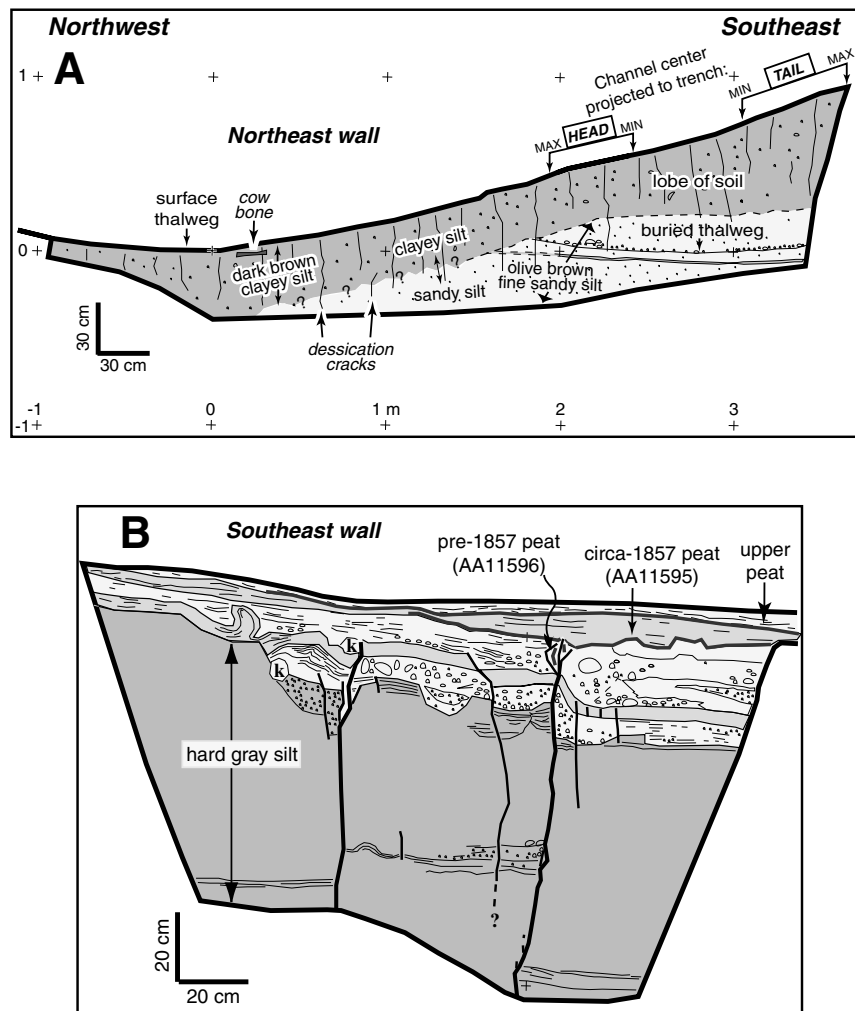


Figure 5. Logs of hand-dug trenches at two sites: (A) 29b2:1 and (B) 107g:11 (i.e., sites 1 and 11 of Sieh, 1978b); locations shown in Figures 3 and 4. In (B): faults, thickest black linework (other than trench outlines); peats shown as thick dark gray lines; k, krotovina or infilled burrow; darkest gray shaded unit indicates material distinctly harder than in overlying units. Units above this are young silts and sands of the major channel. Fine lines indicate laminations and contacts.

For site 107g:11, Lienkaemper agrees almost precisely with Sieh (1978b) on the amount of slip on the main trace ( $4.2 \pm 0.6$  versus  $4.1 \pm 0.9$  m). However, Lienkaemper measured an additional  $2.0 \pm 0.3$  m slip on an adjacent splay (Fig. 4), for a total slip of  $6.2 \pm 0.7$  m. To demonstrate the existence of the second trace, a small trench was dug across the fault, and a peat sample was extracted from a fissure fill associated with the most recent surface rupture (Fig. 5B) was radiocarbon dated. In addition, an undisturbed peat unit directly overlying that rupture was dated. Both dates are indistinguishable from modern carbon and thus are reasonably certain ( $>0.95$  confidence) to reflect the 1857 event and no previous events.

Site 109d:12 is a poorly constrained offset at which one can scale offsets of 3–6 m by photo interpretation (see URL). It is difficult to reproduce any unique measurement on the

ground because slumping and erosion have greatly complicated possible reconstructions of stream channel geomorphology. Sieh (figure 11 in 1978b) indicates many of these complications on his topographic and geomorphic map of this site. Hence, although this site constrains the 1857 slip to smaller than the slip in the Carrizo Plain (ca. 9 m), it is of little use in discriminating the desired details of the 1857 slip near Cholame: that is, 3.5 versus 5.5 m.

Next, let us consider the remaining four sites of the eight used by Sieh and Jahns (1984) in order of decreasing reliability as assigned by Sieh (1978b): 109c:13, 99a2:10, 82c,d:5, and 82a:6 (See URL for 3D imagery). Lienkaemper considered these four sites to be of low reliability, although site 82c,d:5 is distinctly better than the others. Site 109c:13 is a landslide scar apparently offset by the fault. Although the stereoscopic viewpoint chosen by Sieh looks convincing

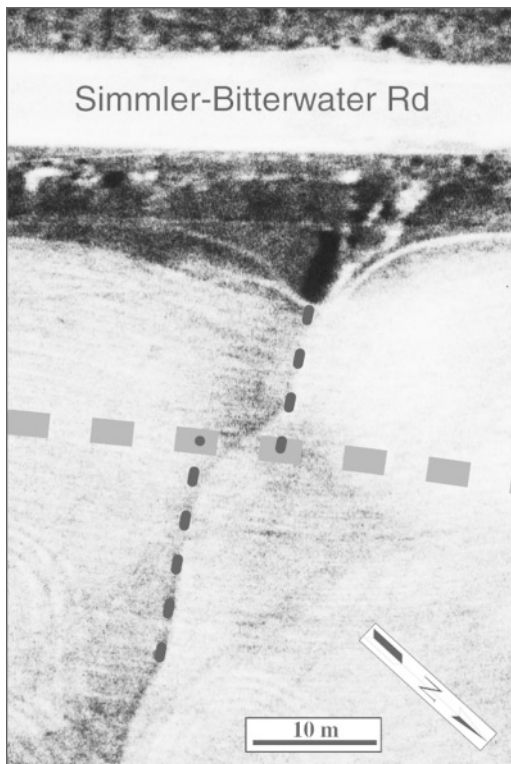


Figure 6. Site 145a (Table 1) shows  $6.7 \pm 0.5$  m of offset in this 1966 USGS WRD aerial photograph (original scale 1:6000). Disking has since destroyed the natural topography.

(see figure 7 in Sieh, 1978b), many other views (especially using an aerial photo image) allow a range of equally convincing interpretations of widely varying amounts of possible slip, including zero, because the exact fault location here is uncertain. At site 99a2:10, the presence of three active fault traces crossing a deeply incised and sinuous channel seriously complicates the interpretation of slip. Sieh (1978b) acknowledged that he measured slip on only one trace of these three and thus it represents only a minimum value. In this study, slip was measured on all three traces and summed, but measurement uncertainties are so large as to make the result of little use. Site 82c,d:5 is complicated by the presence of a second fault trace not noticed by Sieh (1978b), and both traces are poorly expressed. Slumping and erosional effects at site 82a:6 (ranked as only Fair by Sieh, 1978b) are so severe that an extremely wide range of offset estimates are possible.

This study was greatly aided by 1:2400 aerial photography, and the investigation was focused on a 30-km part of the overall 1857 rupture length ( $>300$  km). These advantages made possible the addition of many new sites to those already measured in the reconnaissance work of Sieh (1978b). Only six of these sites were deemed of sufficiently good quality to be reliable indicators of the 1857 slip: sites 145a, 107b, 95a, 43e, 33b4, and 17a. These sites are de-

scribed in Table 1 (see URL for 3D imagery of these sites). Unfortunately, disking eradicated the best of these sites, and the offset is thus only measurable on the 1966 aerial photos (145a, Fig. 6).

In summary, the four sites that rank as high reliability (Table 1: 122a:15, 31a:2, 84a3:8, 145a) best reflect the 1857 slip, and their offsets range from 5.4 to 6.7 m. Additionally, seven sites ranked as moderate reliability (Table 1: 107g:11, 109d:12, 107b, 95a, 43e, 33b4, 17a) appear to represent the 1857 slip. The average of these 11 medium- and high-quality sites is  $5.8 \pm 0.3$  m ( $\pm 1\sigma$ , standard deviation of the mean). Figure 7A shows all offset data plotted versus distance along the fault, with more reliable sites shaded darker. Taken together, all reliable data suggest that the 1857 slip was ca. 6 m. This study does not support the Sieh and Jahns (1984) value of ca. 3.5 m of characteristic slip. Another view of the data, a histogram (Fig. 8), shows a cluster of points at ca. 6 m and no clustering near ca. 3.5 m. The smallest cluster of offsets 0–1 m can all be attributed to creep and Parkfield earthquakes (see discussion of site 29b2:1 described previously). A broad cluster from 10 to 13 m supports the possibility of the repetition of a characteristic earthquake slip of ca. 6 m on this segment (i.e., possibly the accumulation of slip in two ca. 6-m events). However, this conclusion may place too much emphasis on only four reliable offsets and other explanations are possible.

## Discussion

Resolution of a difference in stream channel offset of less than 50% might seem unimportant. However, public interest in the Parkfield Prediction Experiment and its implications for a planned emergency response by six counties to forecast an  $M$  7 earthquake made a significant difference in the interpretation. Thus, a brief summary of these differing interpretations follows. Figure 7B shows the values of slip from this investigation and those of Sieh (1978b) plotted together. At three sites (107g:11, 99a2:10, 82c,d:5) of the eight in Sieh and Jahns' (1984) Cholame-forecast sites (Sieh 1978b: sites 1, 5, 6, 10, 11, 12, 13, 15), considerable slip on secondary fault traces was not included by Sieh. Offset at three other key sites (109d:12, 109c:13, 82a:6) is too ambiguous or poorly constrained to be useful. Offset interpretations depend on how an observer chooses to reconstruct the post-1857 erosional and depositional history, and most sites are too badly degraded and observations too poorly constrained to discriminate the 1857 slip with the 0- to 2-m precision needed. Both Lienkaemper and Sieh considered site 122a:15 as reliable. However, disking modified it before Sieh (1978b) measured it, and it could only be measured reliably on 1966 aerial photos (Lienkaemper and Sturm, 1989). The gully at site 29b2:1 has the overall appearance of minor offset (0–1 m; Fig. 3), except for a deflection near the fault trace, which led to an interpretation of the 3.5-m slip by Sieh (1978b). Trenching supports a much simpler interpretation: a shallow soil lobe covered the gully near the

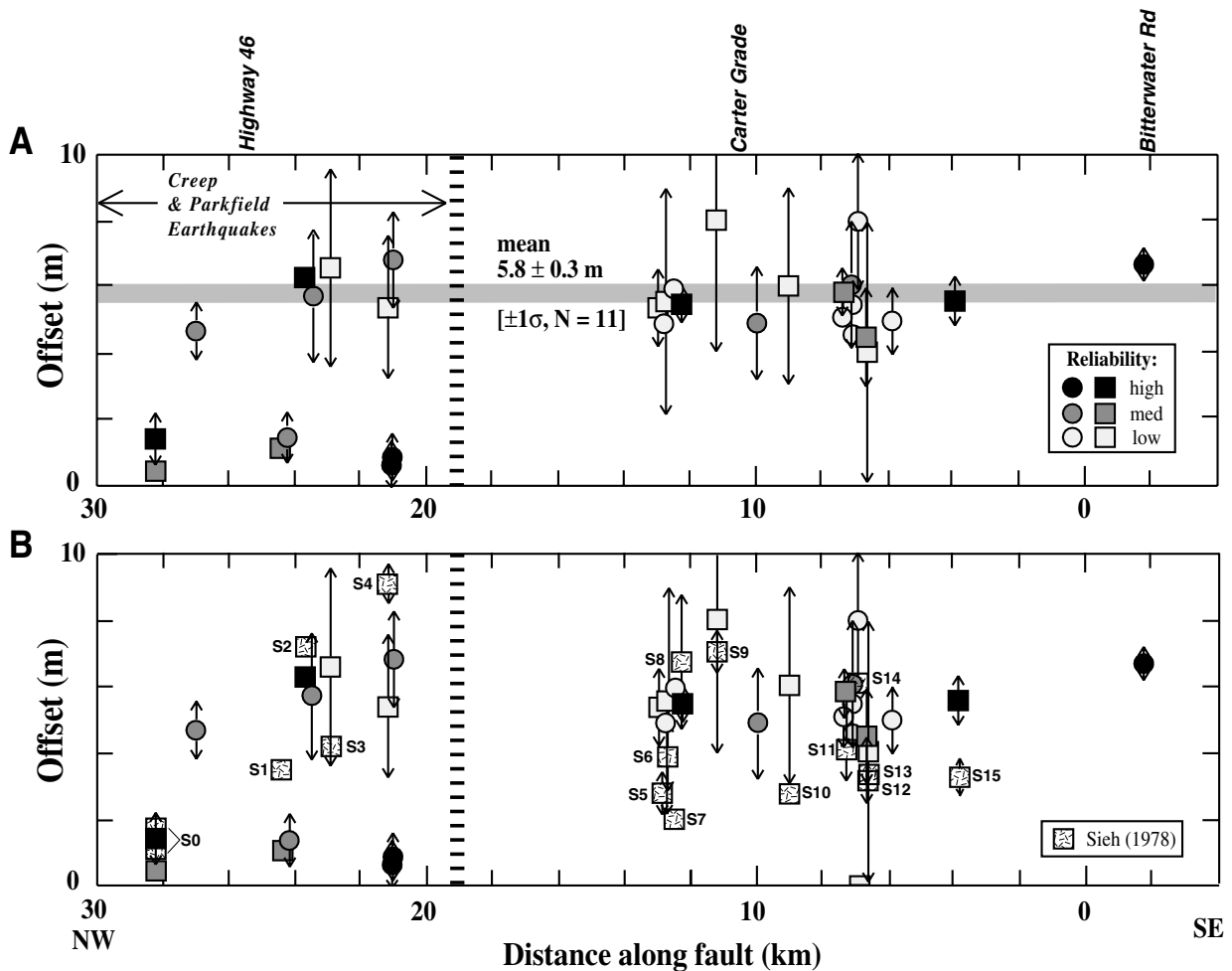


Figure 7. Smallest (<10 m) right-lateral offsets of stream channels southeast of Cholame. (A) Slip data from Table 1 versus distance along the fault from Bitterwater Road. Mean slip for cluster of data of medium and high reliability plotted as gray band at 5.8 m. Squares show results of this study for sites previously measured by Sieh (1978b); circles for new sites. (B) Same data (i.e., from Table 1) and symbols as in (A), but with values of Sieh (1978b) as patterned squares for comparison; numbers indicate site number used by Sieh. Error bars and reliability definitions discussed in text.

fault, either by colluviation or soil creep, and deflected the gully (Fig. 5A). Thus, the entire offset of less than or equal to 1.1 m is most likely an accumulation of creep and slip in moderate Parkfield events and requires no 1857 slip.

This study supplements the data set by adding sites not documented by Sieh (1978b). These additional data support the result of ca. 6-m slip in 1857, and no reliable and complete measurements support the 3–4 m that Sieh and Jahns (1984) suggested as the characteristic slip for this segment.

Although the 1857 slip near Cholame was probably ca. 6 m and not ca. 3.5 m, this does not necessarily lessen the probability of an  $M \geq 7$  earthquake in the next 30 yr. Of the many factors involved, perhaps the most important is the supposed requirement of characteristic slip along a segment because it can be used to infer recurrence times. As discussed previously, this study supports a characteristic slip of ap-

proximately 6 m but does not require characteristic events. Another major question for consideration in earthquake probability is the identification of a distinct Cholame segment. Data from this study do support the existence of a Cholame segment, largely defined as a lower-slip (ca. 6 m) section of the 1857 rupture that adjoins a higher slip region (ca. 9 m) in the Carrizo Plain. The present seismic potential for an  $M \geq 7$  event is widely agreed to exist, although a detailed discussion of the possible segmentation models goes beyond the scope intended for this article (refer instead to Arrowsmith *et al.*, 1997).

## Conclusions

This independent evaluation of stream-channel offsets does not confirm the ca. 3.5-m value of the 1857 slip that

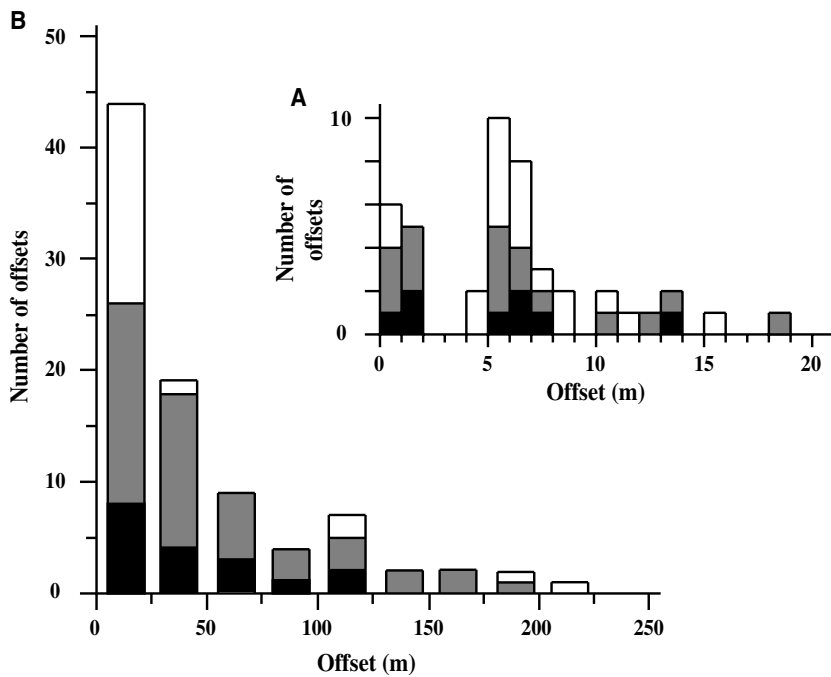


Figure 8. Number of offset stream channels measured versus amount of dextral offset. Data from (A) Table 1 and (B) Tables 1 and 2. Reliability: high (black), medium (gray), low (light gray).

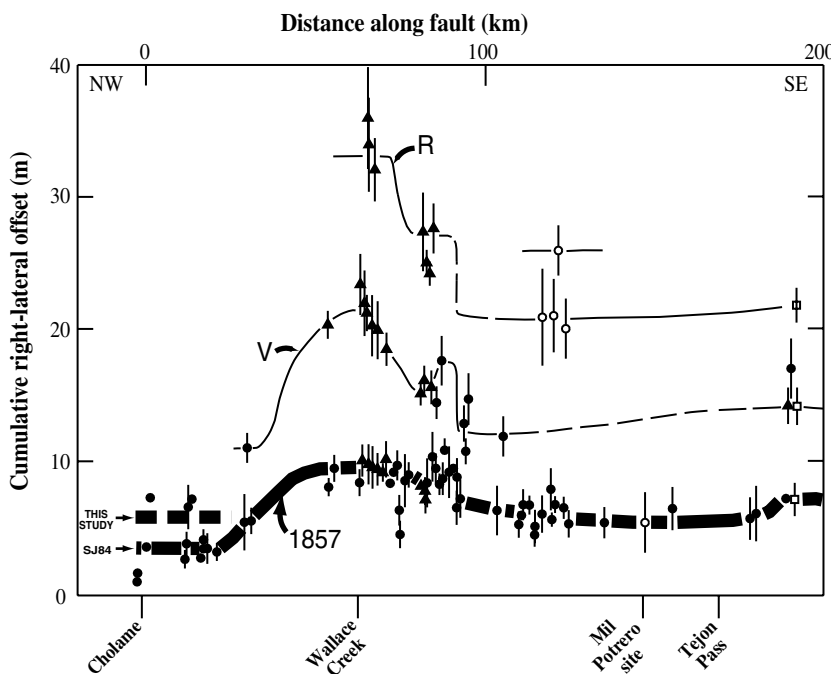


Figure 9. Interpretations of 1857 slip (heavy line labeled SJ84) and previous great earthquakes (V, R) of Sieh and Jahns (1984) between Cholame and Tejon Pass. Slip measurements of Sieh and Jahns (1984) plotted versus distance along the fault southeastward from Highway 46. For comparison, mean slip attributed in this study to 1857 for 30 km southeastward from Cholame (5.8 m, see Fig. 4) shown as dashed heavy line.

Sieh and Jahns (1984) used to forecast an  $M$  7 earthquake for the Cholame segment. Instead, it appears that ca. 6 m of slip may be a more accurate estimate. However, this larger slip (ca. 6 m) is still distinctly lower than the ca. 9 m of slip to the south in Carrizo Plain and still lends plausibility to the existence of a physically distinct segment near Cholame. Based on larger offsets (10–13 m) along this section of the fault, a characteristic earthquake model, that is, repeating ruptures of the ca. 6-m slip near Cholame, is suggested but not required (Fig. 8A). For offsets greater than 20 m (Table

2, Fig. 8) the error in measurement and the decreasing numbers of these offsets precludes further deductions about any earlier characteristic events. The seismic potential for a Cholame segment already exceeds  $M$  7. Assuming a characteristic slip model applies, this study's revised 1857 slip (i.e., 5.8 m/0.034 m/yr) suggests a mean recurrence interval of 170 yr. Thus, the mean recurrence time (2027 = 1857 + 170 yr) now lies within the 30-yr window generally used for probability calculations. Therefore, this segment still appears to have one of the highest probabilities in the state for

an  $M \geq 7$  earthquake, regardless of one's choice in modeling assumptions.

### Acknowledgments

The USGS National Earthquake Hazard Reduction Program (9910-04192) funded the investigation; USGS-CDMG Joint Funding Agreement for the Parkfield Experiment (California Assembly Bill 938) paid for low-sun aerial photography and precision photogrammetry by the USGS Western Mapping Center. W. H. Bakun and A. G. Lindh suggested measuring the 1857 Cholame offsets independently to evaluate the hypothesis of Sieh and Jahns (1984). The author gratefully acknowledges the seven colleagues who gave a thorough field review: M. M. Clark, D. P. Schwartz, R. V. Sharp, J. D. Sims, E. Tsukuda, R. E. Wallace, and especially T. C. Hanks, who orchestrated and drafted the Cholame Eight consensus document for submission to the NEPEC. Special thanks go to K. Sieh for graciously agreeing to join us in Menlo Park to discuss and cosign the consensus document, thus making us the Cholame Nine. Further special thanks go to H. Stenner, S. Hecker, K. Sieh, and an anonymous reviewer for their detailed reviews that substantially improved this article.

### References

- Agnew, D. C., and K. E. Sieh (1978). A documentary study of the felt effects of the great California earthquake of 1857, *Bull. Seism. Soc. Am.* **68**, 1717–1729.
- Andrews, R. (1992). The Parkfield earthquake prediction of October 1992; the emergency services response, *Earthquakes Volcanoes* **23**, 170–174.
- Arrowsmith, R., K. McNally, and J. Davis (1997). Potential for earthquake rupture and  $M 7$  earthquakes along the Parkfield, Cholame, and Carrizo segments of the San Andreas Fault, *Seism. Res. Lett.* **68**, 902–916.
- Bakun, W. H., and A. G. Lindh (1985a). The Parkfield, California, prediction experiment, in *Minutes of the National Earthquake Prediction Council*, November 16–17, 1984, C. F. Shearer (Editor), *U.S. Geol. Surv. Open-File Rept.* 85–201. 16–55.
- Bakun, W. H., and A. G. Lindh (1985b). The Parkfield, California, earthquake prediction experiment, *Science* **229**, 619–624.
- Bakun, W. H., and T. V. McEvilly (1984). Recurrence models and Parkfield, California, earthquakes, *J. Geophys. Res.* **89**, 3051–3058.
- Bakun, W. H., K. S. Breckenridge, J. D. Bredehoeft, R. O. Burford, W. L. Ellsworth, M. J. S. Johnston, L. M. Jones, A. G. Lindh, C. E. Mortensen, R. J. Mueller, C. M. Poley, E. A. Roeloffs, S. S. Schulz, P. Segall, and W. Thatcher (1987). Parkfield, California, earthquake prediction scenarios and response plans, *U.S. Geol. Surv. Open-File Rept.* 87–192, 59 pp.
- Ben-Zion, Y., J. R. Rice, and R. Dmowska (1993). Interaction of the San Andreas Fault creeping segment with adjacent great rupture zones and earthquake recurrence at Parkfield, *J. Geophys. Res.* **98**, 2135–2144.
- Brown, R. D. Jr., and R. E. Wallace (1968). Current and historic fault movement along the San Andreas fault between Paicines and Camp Dix, California, in *Conference on Geologic Problems of San Andreas Fault System, Stanford, California, 1967. Proc. Stanford Univ. Publ. Geol. Sci.* **11**, 22–39.
- Burford, R. O., and P. W. Harsh (1980). Slip on the San Andreas fault in central California from alignment array surveys, *Bull. Seism. Soc. Am.* **70**, 1233–1261.
- California OES (1988). *Parkfield Earthquake Prediction Response Plan*. State of California OES, Sacramento, California, 19 pp.
- Davis, P. M., D. D. Jackson, and Y. Y. Kagan (1988). The longer it has been since the last earthquake, the longer the expected time until the next? (abstract), *EOS Trans. Am. Geophys. Union* **69**, 1299 pp.
- Jackson, D. D., and Y. Y. Kagan (1998). Parkfield earthquake; not likely this year (abstract), *Seism. Res. Lett.* **69**, 151.
- Johnson, H. R. (1905). *Field notebook 3354. U.S. Geol. Surv. Archiv.*, Denver, Colorado, 67 pp.
- Kagan, Y. Y. (1997). Statistical aspects of Parkfield earthquake sequence and Parkfield prediction experiment, *Tectonophysics* **270**, 207–219.
- Lindh, A. G., and M. R. Lim (1995). A clarification, correction, and updating of Parkfield, California, earthquake prediction scenarios and response plans, *U.S. Geol. Surv. Open-File Rept.* 87–192, 39 pp.
- Lienkaemper, J. J. (1987). 1857 slip on the San Andreas Fault southeast of Cholame, California (abstract), *EOS Trans. Am. Geophys. Union* **68**, 1345.
- Lienkaemper, J. J., and T. A. Sturm (1989). Reconstruction of a channel offset in 1857(?) by the San Andreas Fault near Cholame, California, *Bull. Seism. Soc. Am.* **79**, 901–909.
- Lienkaemper, J. J., and W. H. Prescott (1989). Historic surface slip along the San Andreas Fault near Parkfield, California, *J. Geophys. Res.* **94**, 17,647–17,670.
- Michael, A. J., and L. M. Jones (1998). Seismicity alert probabilities at Parkfield, California, revisited, *Bull. Seism. Soc. Am.* **87**, 117–130.
- Miller, S. A. (1996). Fluid-mediated influence of adjacent thrusting on the seismic cycle at Parkfield, *Nature* **382**, 799–802.
- NEPECCWG (1994). Earthquake research at Parkfield, California, 1993 and beyond; report of the National Earthquake Prediction Evaluation Council (NEPEC) working group to evaluate the Parkfield earthquake prediction experiment, *U.S. Geol. Surv. Circ.* **1116**, 14 pp.
- Roeloffs, E., and J. Langbein (1994). The earthquake prediction experiment at Parkfield, California, *Rev. Geophys.* **32**, 315–336.
- Savage, J. C. (1991). Criticism of some forecasts of the National Earthquake Prediction Evaluation Council, *Bull. Seism. Soc. Am.* **81**, 862–881.
- Savage, J. C. (1993). The Parkfield prediction fallacy, *Bull. Seism. Soc. Am.* **83**, 1–6.
- Sieh, K. E. (1978a). Central California foreshocks of the great 1857 earthquake, *Bull. Seism. Soc. Am.* **68**, 1731–1749.
- Sieh, K. E. (1978b). Slip along the San Andreas Fault associated with the great 1857 earthquake, *Bull. Seism. Soc. Am.* **68**, 1421–1447.
- Sieh, K. E., and R. H. Jahns (1984). Holocene activity of the San Andreas Fault at Wallace Creek, California, *Geol. Soc. Am. Bull.* **95**, 883–896.
- Stuart, W. D., R. J. Archuleta, and A. G. Lindh (1985). Forecast model for moderate earthquakes near Parkfield, California, *J. Geophys. Res.* **90**, 592–604.
- Working Group on California Earthquake Probabilities (1988). Probabilities of large earthquakes occurring in California on the San Andreas fault, *U.S. Geol. Surv. Open-File Rept.* OF 88–398, 62 pp.

U.S. Geological Survey 977  
Menlo Park, California 94025  
jlienka@usgs.gov

Manuscript received 9 March 2000.